



Preparation and Characterization of Poly Lactide and Poly (Butylene Adipate-co-Terephthalate) Nanocomposites Reinforced with Graphene Nanoplatelet

Sima Kashi, Rahul K. Gupta, Nhol Kao and Sati N. Bhattacharya

Rheology and Materials Processing Centre (RMPC), School of Engineering, RMIT University, Melbourne, Victoria 3000, Australia

With excellent characteristics including high mechanical and electrical properties, graphene nanoplatelets (GNPs) can be used for reinforcing polymers and developing novel materials. In the current study, different concentrations of GNPs were embedded in poly lactide and poly (butylene adipate-co-terephthalate). Morphology of the nanocomposites was studied via scanning electron microscopy and X-Ray diffraction. Effects of GNP loading on electrical, mechanical and thermal properties of the two matrices were determined. Results showed significant enhancement in electrical conductivity, mechanical strength and thermal stability of both polymers with addition of GNPs.

1. Introduction

With the increase in public consciousness towards environmental friendly materials, biodegradable polymers have received significant attention in recent years as alternatives for replacing the persistence commercial polymers in various applications and products. Poly lactide (PLA) and poly(butylene adipate-co-terephthalate) (PBAT) are among the leading biodegradable polymers derived from biosources and petroleum, respectively [1]. However, in spite of their appealing properties, these two polymers have some disadvantages such as PLA's slow rate of crystallization and low thermal stability [2] and PBAT's insufficient mechanical strength [3]. These drawbacks limit the applicability of PLA and PBAT. A practical way to overcome the shortcomings of PLA and PBAT is to incorporate nano-sized fillers in the matrix, similar to what has been done for commercial polymers such as polyethylene [4], polypropylene [5] and polystyrene [6]. Nano-fillers are more effective reinforcements than their conventional counterparts because a smaller amount of nanoparticles could result in a larger enhancement in the mechanical, electrical and thermal properties of polymer matrix [7].

In the present study, different concentrations of graphene nanoplatelets (GNPs) were dispersed in PLA and PBAT via melt-mixing and compression moulding. Effects of GNPs on morphology, electrical and mechanical properties as well as thermal stability of PLA and PBAT were determined.

2. Experimental

2.1 Materials

Poly lactide (4032D) with density of 1.24 g/cm³ and melting point of 160 °C was purchased from NatureWorks LLC. PBAT was Ecoflex F Blend C1200 (BASF, Germany) with density of 1.25-1.27 g/cm³ and melting range of 110-120 °C. "M" grade GNPs were obtained from XG Sciences (USA) which exhibit an average thickness of 6–8 nm, surface area of 120–150 m²/g and density of 2.2 g/cm³.

2.2 Nanocomposites Preparation

PLA/GNP and PBAT/GNP nanocomposites were prepared in an internal mixer (Haake Rheomix OS R600) with roller rotors operated at 60 rpm for a mixing time of 10 min at 180 °C and 140 °C for PLA and PBAT nanocomposites, respectively. Nanocomposites were prepared with six different GNP concentrations (0, 3, 6, 9, 12, 15 wt%). The PLA/GNP and PBAT/GNP samples were then compression moulded at 180 °C and 140 °C respectively with a compression force of 80 kN for 5 min.

2.3 Characterization

A FEI Quanta200 scanning electron microscope was used to study the morphology of fractured surfaces of the nanocomposites. For samples with up to 6 wt% GNPs, accelerating voltage was fixed at 5 kV to avoid charging and for nanocomposites with higher GNP loadings, it was set to 10 kV. X-ray diffraction (XRD) tests were conducted at ambient temperature using a Bruker D4 ENDEAVOR diffractometer with LynxEye detector. The X-ray beam was nickel-filtered Cu-K α with a wavelength of 1.54 Å, operated at a generator voltage of 40 kV and a current of 35 mA. AC conductivity was determined from electrical permittivity values of the samples, which were extracted from their scattering parameters collected by using a vector network analyser (Wiltron 37269A) with waveguide setup over X-band frequency range (8.2-12.4 GHz). Thermal gravimetric analysis tests were conducted using a Perkin Elmer TGA (STA 6000). Samples were first stabilised at 50 °C for 2 minutes and then heated up to 900 °C under a nitrogen atmosphere at heating rates of 10 °C /min. Instron 4467 Universal testing machine was used to measure the tensile properties according to ASTM D638M with a crosshead speed rate of 1 and 5 mm/min for PLA and PBAT nanocomposites, respectively.

3. Results

3.1 Morphology

SEM images of PLA and PBAT nanocomposites with 3 wt% GNPs are presented in Fig. 1. More layers of graphene are stacked together in PLA than in PBAT. Furthermore, bigger voids are observed between the platelets and PLA than between GNPs and PBAT indicating the weaker adhesion of PLA to the platelets compared to PBAT. Therefore, it is observed that GNPs are better dispersed in PBAT than in PLA; This observation is in agreement with a previous research [8]. It is also interesting that in a study on dispersion of CNTs in a blend of PLA and PBAT, higher affinity was detected between the nanotubes and PBAT [9]. The authors attributed this to the chemical structure of PBAT containing aromatic molecules [9].

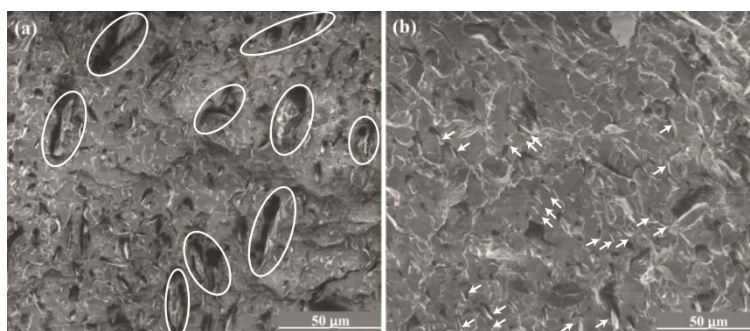


Fig. 1. Dispersion states of GNPs in the two polymers: SEM images of (a) PLA and (b) PBAT nanocomposites with 3wt% GNPs.



Fig. 2 shows that the position of GNPs' peak of 26.5° (002) is not changed noticeably in both types of nanocomposites, indicating that the spacing between graphene platelets in the nanocomposites has not increased (Bragg's law) noticeably. However, the intensity of this peak increases with increasing GNP loading, as expected. Comparing the diffraction patterns of PBAT/GNP nanocomposites with pure PBAT demonstrates that addition of GNPs has not appreciably affected the semi-crystalline structure of the polymer. On the hand, the increase in PLA's peak of $2\theta \sim 16.7^\circ$ in PLA/GNP nanocomposites shows enhancement of crystallinity of PLA due to presence of GNPs.

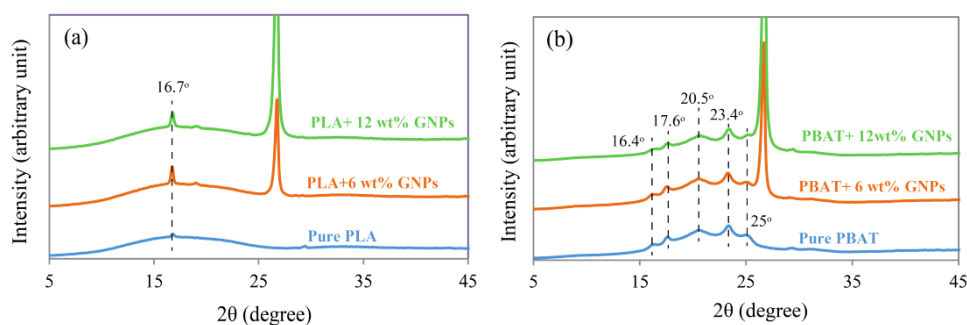


Fig. 2. X-ray diffraction patterns of (a) PLA and (b) PBAT nanocomposites.

3.2 Electrical Conductivity

The variation of AC conductivity (σ) of PLA and PBAT nanocomposites as a function of GNP loading is plotted in Fig. 3. It is observed that conductivities of both polymers increase markedly with GNP loading. It is interesting to note that while up to 6 wt% GNPs PLA and PBAT nanocomposites have comparable conductivities, at higher graphene contents, PLA nanocomposites show better conductivity. This difference is attributed to the better formation of conductive pathways of graphene platelets within PLA due to non-uniform GNP dispersion as compared to PBAT.

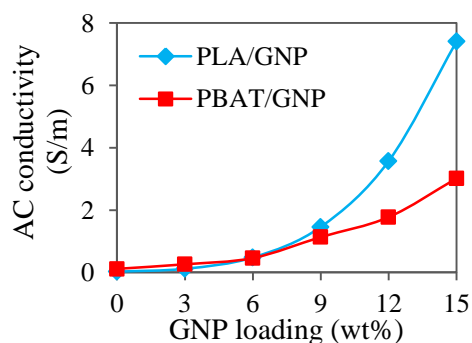


Fig. 3. AC conductivity vs. GNP loading at 10 GHz.

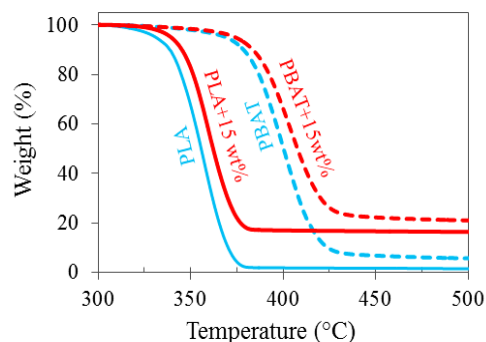


Fig. 4. TGA curves of pure PLA and PBAT and their 15wt% GNP nanocomposites.

3.3 Thermal Stability

Effect of GNP embedding on thermal stability of PLA and PBAT was determined via thermogravimetric analysis (TGA) under nitrogen. The onset thermal degradation of pure PLA is detected to be around 315°C (1% weight loss) which is in good agreement with previously reported data on the same PLA grade. The degradation of neat PLA is completed at about 380°C . With a higher onset degradation temperature, 338°C , and a wider thermal degradation window ($338\text{--}426^\circ\text{C}$) unfilled PBAT is thermally more stable than PLA. As it is



evident from Fig. 4, addition of GNPs enhances the thermal stability of both PLA and PBAT markedly.

3.4 Young's Modulus

Young's moduli of PLA and PBAT nanocomposites were normalised against the moduli of unfilled PLA and PBAT, respectively. Results is summarised in Table 1. Pristine PLA and PBAT have Young's moduli of about 2980 and 96 MPa, respectively. Addition of GNPs improves the moduli of both matrices. This improvement is due to the very high intrinsic mechanical characteristics of GNPs as well as their high aspect ratio. Highest values of moduli for PLA and PBAT are observed at 9 and 15 wt% GNPs, respectively. The decrease in modulus of PLA/GNP nanocomposites with GNP loadings of above 9 wt% could be due to the weak interfacial bonding between the nanoplatelets and PLA. Agglomeration of GNPs at such high concentrations could result in formation of weak points in the material, leading to lower modulus.

Table 1. Normalised Young's Modulus of PLA and PBAT nanocomposites.

GNP wt%	0	3	6	9	12	15
PBAT/GNP	1.0	1.5	2.5	2.9	3.7	4.8
PLA/GNP	1.0	1.1	1.4	2.1	1.8	1.7

4. Conclusions

Biodegradable PLA/GNP and PBAT/GNP nanocomposites were prepared with up to 15 wt% GNPs. Scanning electron micrographs showed good dispersion of the platelets in PBAT. XRD tests revealed that the spacing between the platelets in the nanocomposites was not much affected by high shearing during melt-mixing. As expected, electrical conductivity of both PLA and PBAT were significantly enhanced with GNP addition. Furthermore, thermal stabilities of the matrices increased with increasing GNP concentration. The highest Young's moduli were obtained at 9 and 15 wt% of GNPs for PLA and PBAT nanocomposites, respectively.

References

- [1] Jiang L, Wolcott MP and Zhang J 2006 *Biomacromolecules* **7** 199
- [2] Chieng B, Ibrahim N, Yunus W and Loo Y 2014 *Polymers* **6**(8) 2232
- [3] Ecoflex F blend C1200 Data sheet. Available from:
http://www.plasticsportal.net/wa/plasticsEU~tr_TR/function/conversions:/publish/common/upload/biodegradable_plastics/Ecoflex_F_Blend_C1200.pdf
- [4] Jiang X, Drzal L T 2011 *Composites Part A: Applied Science and Manufacturing* **42**(11) 1840
- [5] Garzon C, Wilhelm M, Abbasi M and Palza H 2016 *Macromol. Mater. Eng.* **301**(4) 429
- [6] Rohini R and Bose S 2014 *ACS Appl. Mater. Interfaces* **6**(14) 11302
- [7] Hussain F, Hojjati M, Okamoto M and Gorga R E 2006 *J. Compos. Mater.* **40**(17) 1511
- [8] Mittal V, Chaudhry A U and Luckachan G E 2014 *Mater. Chem. Phys.* **147**(1-2) 319
- [9] Ko S W, Gupta R K, Bhattacharya S N and Choi H J 2010 *Macromol. Mater. Eng.* **295**(4) 320